CHAPTER 82

Nonlinear Refraction-Diffraction of Surface Waves over Arbitrary Depths

Serdar Beji[1] and Kazuo Nadaoka[2]

Abstract

A nonlinear dispersive wave model recently introduced by the authors is used for sample simulations of directional wave transformations over gently varying depths. Various forms of the generic equation are presented first, and the dispersion and nonlinear characteristics of the model are investigated analytically. Following the numerical descriptions, the experimental data for linear wave propagation over a circular shoal and for nonlinear wave propagation over a topographical lens are compared to the model predictions with satisfactory agreements. Finally, as a demonstration of the unified character of the model, the unidirectional version of the wave equation is implemented for simulating the gradual transformation of an initially second-order Stokes wave train over decreasing depth into a cnoidal wave train.

Introduction

The mean wave-number of a wave field propagating from deep to shallow water changes gradually and, when subject to spatial non-uniformities and non-linearity, causes quite profound modifications in the overall wave pattern. For an accurate description of such phenomena it is essential that a good wave model accommodates the relevant physical mechanisms. One such a model is Berkhoff's (1972) mild-slope equation, which has been used successfully in the last two and half decades. The model however has a few shortcomings, notably its restriction to linear, monochromatic waves. The time-dependent form of this equation (Smith and Sprinks, 1975) performs better in representing a narrow-banded wave field but cannot account for nonlinear effects which are quite appreciable for waves propagating on shallow waters or over sand-bars (Freilich and Guza 1984, Byrne 1969, Young 1989). In the nearshore zone the Boussinesq-type models are probably the best choice; however, their weak

[1] Assoc. Prof., Department of Naval Architecture and Ocean Engineering, Istanbul Technical University, Maslak 80626, Istanbul, Turkey

[2] Professor, Graduate School of Information Science and Engineering, Tokyo Institute of Technology, 2-12-1 O-okayama, Meguro-ku, Tokyo 152, Japan

dispersion characteristics imposes limits on the applicable range of these equations. Despite the successful reports of extending their validity range (Witting 1984, Madsen *et al.* 1991, Nwogu 1993, Beji and Nadaoka, 1996), due to the certain assumptions introduced in their derivation, they remain finite-depth equations. The existing wave models then provide only partial representations of the observed effects: the mild-slope type equations are usable only for linear, narrow-banded waves while the Boussinesq equations are restricted by their applicable depth.

In order to overcome the drawbacks of the available wave models; namely, the linearity, narrow-bandedness, and depth-limitation, Nadaoka *et al.* (1994, 1997) advanced a new approach which was termed as the *multiterm-coupling technique*. They expressed the velocity field as a sum, each term comprising a hyperbolic vertical-dependence function and a corresponding velocity vector independent of depth. This expression was then used in nonlinear forms of the depth-integrated continuity and momentum equations in conjunction with the Galerkin procedure which ensured the solvability. The result was a set of wave equations that could describe the evolutions of a broad-banded nonlinear wave field propagating over arbitrary depths. These general equations have been shown to produce the aforementioned well-known wave models as degenerate cases besides generating the second-order Stokes waves on deep water. Here, the single-component (*i.e.*, a single-term expansion of the velocity field) equations in combined form as given by Beji and Nadaoka (1997) is used.

Wave Model and Its Various Forms

Nadaoka *et al.* (1997) give the following continuity and momentum equations as the single-component wave model, correct to the second-order in nonlinearity:

$$\eta_t + \nabla \cdot \left[\left(\frac{C_p^2}{g} + \eta \right) \mathbf{u} \right] = 0, \tag{1}$$

$$C_p C_g \mathbf{u}_t + C_p^2 \nabla \left[g\eta + \eta w_t + \frac{1}{2} \left(\mathbf{u} \cdot \mathbf{u} + w^2 \right) \right]$$
$$= \frac{C_p(C_p - C_g)}{k^2} \nabla (\nabla \cdot \mathbf{u}_t) + \nabla \left[\frac{C_p(C_p - C_g)}{k^2} \right] (\nabla \cdot \mathbf{u}_t), \tag{2}$$

where η is the free surface displacement, $\mathbf{u}(u, v)$ the two-dimensional horizontal velocity vector and w the vertical component of the velocity both at the still water level $z = 0$. C_p, C_g, and k are respectively the phase and group velocities, and wave-number computed according to linear theory for a prescribed incident frequency ω and a local depth h. g is the gravitational acceleration, ∇ stands for the horizontal gradient operator with components $(\partial/\partial x, \partial/\partial y)$, and subscript t indicates partial differentiation with respect to time. Note that (1) and (2) are formulated for varying depth and therefore C_p, C_g, and k are in general spatially varying quantities. The above single-component equations may be considered as evolution equations that can simulate weakly-nonlinear, narrow-banded wave transformations over arbitrary depths. Compared with the Boussinesq-type equations, these equations are superior in the sense that they may be used without any restriction on the depth.

Eliminating **u** from (1) and (2) to obtain a wave equation for the surface displacement η results in (Beji and Nadaoka, 1997):

$$
\begin{aligned}
&C_g \eta_{tt} - C_p^3 \nabla^2 \eta - \frac{(C_p - C_g)}{k^2} \nabla^2 \eta_{tt} - C_p \nabla(C_p C_g) \cdot \nabla \eta \\
&- \frac{3}{2} g C_p \left(3 - 2 \frac{C_g}{C_p} - \frac{k^2 C_p^4}{g^2} \right) \nabla^2 \left(\eta^2 \right) = 0.
\end{aligned}
\tag{3}
$$

Equation (3), named as the *time-dependent nonlinear mild-slope equation*, is the wave model adopted in this work. For a prescribed wave frequency and a definite water depth the wave number and the phase and group celerities are determined according to the relations given by linear theory.

Instead of eliminating the velocity field, invoking the existence of a two-dimensional potential function at the still water level $z = 0$ such that $\mathbf{u} = \nabla \phi$ and eliminating the surface elevation from (1) and (2), one obtains

$$
\begin{aligned}
&C_g \phi_{tt} - C_p^3 \nabla^2 \phi - \frac{(C_p - C_g)}{k^2} \nabla^2 \phi_{tt} - C_p \nabla(C_p C_g) \cdot \nabla \phi \\
&+ \frac{3}{2} C_p \left(1 - \frac{k^2 C_p^4}{g^2} \right) \left[(\nabla \phi)^2 \right]_t = 0,
\end{aligned}
\tag{4}
$$

where the obvious approximation $(\nabla \phi)^2 \simeq -k^2 \phi^2$ in the nonlinear term is intentionally avoided since ϕ itself is not a directly measurable physical quantity and cannot be specified uniquely in the computations. Note also that for infinitely deep water waves $C_p^2 = g/k$ hence the coefficient of the nonlinear term in (4) vanishes, indicating a linear velocity potential for the second-order waves as in the Stokes second-order theory. The surface displacement on the other hand remains nonlinear regardless of the relative depth.

The linearized form of (3) or (4) is comparable with the time-dependent mild-slope equation of Smith and Sprinks (1975) but equation (3) can simulate a relatively broader wave spectrum as shown by Beji and Nadaoka (1997).

It is possible to extract from (3) a wave equation describing only the one-dimensional, right-going waves (Beji and Nadaoka, 1997):

$$
\begin{aligned}
&C_g \eta_t + \frac{1}{2} C_p (C_p + C_g) \eta_x - \frac{(C_p - C_g)}{k^2} \eta_{xxt} - \frac{C_p(C_p - C_g)}{2k^2} \eta_{xxx} \\
&+ \frac{1}{2} \left[C_p(C_g)_x + (C_p - C_g)(C_p)_x \right] \eta + \frac{3}{4} g \left(3 - 2 \frac{C_g}{C_p} - \frac{k^2 C_p^4}{g^2} \right) \left(\eta^2 \right)_x = 0,
\end{aligned}
\tag{5}
$$

which may be shown to include the KdV equation as a special case as well as admitting the second-order Stokes waves as solution in deep water.

The counterpart of (5) in terms of the one-dimensional potential is

$$
\begin{aligned}
&C_g \phi_t + \frac{1}{2} C_p (C_p + C_g) \phi_x - \frac{(C_p - C_g)}{k^2} \phi_{xxt} - \frac{C_p(C_p - C_g)}{2k^2} \phi_{xxx} \\
&+ \frac{1}{2} \left[C_p(C_g)_x + (C_p - C_g)(C_p)_x \right] \phi + \frac{3}{4} C_p \left(1 - \frac{k^2 C_p^4}{g^2} \right) (\phi_x)^2 = 0.
\end{aligned}
\tag{6}
$$

It should be remarked that the linear dispersion characteristics of (5) and (6) are better than those of (3) and (4). More specifically, (5) and (6) can simulate waves with broader spectral width than the generic equations (3) and (4). The details on the subject will be reported separately.

Solitary and Stokes Second-Order Waves

It has already been indicated that the wave model provides a unified approach in describing the nonlinear waves at arbitrary water depths. Simple analytical investigations are now presented to clarify the nonlinear characteristics of the model regarding the solitary and Stokes second-order waves. We begin with the solitary waves.

Let us seek a solution of the form $\eta = H \cosh^{-2}[(x \pm C_s t)/l_s]$, where H is the prescribed wave height, l_s and C_s are respectively the length scale and the phase speed of the solitary wave which are yet unknown quantities to be determined from the wave equation (3). The form adopted is the lowest-order solution, the general expression is an infinite sum of hyperbolic cosine functions of higher powers (see Fenton, 1972); for the present purposes however it will suffice. Substituting this expression in (3) and solving for l_s and C_s give

$$l_s = \left[\frac{6(C_p - C_g)\left(C_p^2 + \frac{2}{3}\beta H\right)}{\beta k^2 C_g H}\right]^{1/2}, \qquad C_s = \left[\frac{C_p}{C_g}\left(C_p^2 + \frac{2}{3}\beta H\right)\right]^{1/2} \qquad (7)$$

where $\beta = \frac{3}{2}g\left(3 - 2\frac{C_g}{C_p} - \frac{k^2 C_p^4}{g^2}\right)$ is the coefficient of the nonlinear term in (3) divided by C_p. A matter of historic interest is obvious from the form of l_s. It becomes zero for $C_p = C_g$; that is, nonlinear-nondispersive waves cannot maintain a permanent form simply because there exists no dispersivity to counterbalance the steepening action of nonlinearity. However, allowing the lowest-order dispersion by letting $C_p \simeq (gh)^{1/2}(1 - k^2 h^2/6)$ and $C_g \simeq (gh)^{1/2}(1 - k^2 h^2/2)$, as in the Boussinesq theory, is sufficient to obtain a permanent form. If these approximate forms are used in (7) and the higher-order dispersion contributions are dropped,

$$l_s \simeq \left[\frac{4h^3(1 + H/h)}{3H}\right]^{1/2}, \qquad C_s \simeq [g(h + H)]^{1/2}, \qquad (8)$$

which are in complete agreement with the classical expressions (Miles, 1980). l_s is the same as Rayleigh's (1876) result and for small H/h it may be replaced with $(4h^3/3H)^{1/2}$, which is the well-known expression.

Assuming that the wave equation (3) admits the second-order Stokes waves as solution we let $\eta = a\cos(k_s x \pm \omega t) + b\cos 2(k_s x \pm \omega t)$ and substitute this expression into (3) to determine the unknown wave number k_s and the second-harmonic amplitude b. The primary wave amplitude a and the frequency ω are taken to be known. Equating the zeroth- and first-order terms to zero gives

$$k_s^2 = k^2, \qquad b = \frac{\beta a^2}{6C_p(C_p - C_g)}, \qquad (9)$$

where the interaction of the primary wave with the second-harmonic is excluded in the above analysis to be consistent with the perturbation approach of Stokes. Note, for deep water waves $C_p = (g/k)^{1/2}$, $C_g = C_p/2$, and $\beta = \frac{3}{2}g$ hence $b = \frac{1}{2}ka^2$, which is the same as the second-order Stokes theory predicts.

Equation (3) is an evolution equation and therefore, unlike a sharply truncated perturbation solution, produces higher-order nonlinear dispersion effects which are partially correct. If the term produced through the interaction of the primary wave with the second-harmonic is retained, k_s becomes

$$k_s^2 = k^2 \left(1 + \frac{\beta b}{C_p C_g} \right)^{-1}, \tag{10}$$

where b is as given in (9). For infinitely deep water waves equation (10) may be approximately written as $k_s \simeq (1 - \frac{3}{4}k^2a^2)k$, which is slightly at variance with the Stokes' third-order result $k_s \simeq (1 - k^2a^2)k$ (approximated for small ka). We may then conclude that the partially correct third-order nonlinear effects produced by essentially second-order wave equation (3) is a good approximation to the Stokes third-order theory. This point has been verified through numerical simulations as well (Beji and Nadaoka, 1997).

Numerical Modeling

Equation (3) is first manipulated into the following form:

$$n\eta_{tt} - C_p^2 \nabla^2 \eta - \frac{C_p^2(1-n)}{\omega^2}\nabla^2\eta_{tt} - \nabla(nC_p^2) \cdot \nabla\eta$$
$$- \frac{3}{2}g \left(3 - 2n - \frac{\omega^2 C_p^2}{g^2} \right) \nabla^2 \left(\eta^2 \right) = 0, \tag{11}$$

where ω is the prescribed dominant wave frequency and $n = C_g/C_p$. Compared with (3) equation (11) is computationally preferable as it requires the storage of only n and C_p (or C_p^2) over the computational domain instead of k, C_p, C_g. Three-time-level centered finite difference approximations were used for the discretization of (11) which resulted in implicit schemes both in x- and y-directions. The three-point-averaging formulation of Zabusky and Kruskal (1965) was used in evaluating the spatial derivatives of the nonlinear terms, as it improved the robustness of the scheme. For computational efficiency an iterative approach was adopted and the domain was swept in the x- and y-directions separately, treating the crosswise new time level variables known by using the last available values. Giving only the time derivatives in discretized form, the x-sweep equation is

$$n\frac{\left(\eta^{k+1} - 2\eta^k + \eta^{k-1}\right)}{\Delta t^2} - \frac{C_p^2(1-n)}{\omega^2}\frac{\left(\eta_{xx}^{k+1} - 2\eta_{xx}^k + \eta_{xx}^{k-1}\right)}{\Delta t^2}$$
$$= \frac{C_p^2(1-n)}{\omega^2}\frac{\left(\eta_{yy}^{k+1} - 2\eta_{yy}^k + \eta_{yy}^{k-1}\right)}{\Delta t^2} + C_p^2\left(\eta_{xx}^k + \eta_{yy}^k\right)$$
$$+ \left(nC_p^2\right)_x \eta_x^k + \left(nC_p^2\right)_y \eta_y^k + \frac{3}{2}g\left(3 - 2n - \frac{\omega^2 C_p^2}{g^2}\right)\left[\left(\bar{\eta}^k\bar{\eta}^k\right)_{xx} + \left(\bar{\eta}^k\bar{\eta}^k\right)_{yy}\right], \tag{12}$$

in which the superscript k denotes the time level and $\bar{\eta}^k = (\eta_{i+1,j}^k + \eta_{i,j}^k + \eta_{i-1,j}^k)/3$ with i and j denoting the spatial nodes in the x and y- directions, respectively. The new time level values η_{yy}^{k+1}'s appearing on the right-hand side of (12) are treated as known by using the last computed values so that η^{k+1} and η_{xx}^{k+1}'s appearing on the left-hand side are the only unknowns. The resulting matrix equation is tridiagonal and can be solved quite efficiently.

Similarly, the y-sweep equation is

$$n\frac{\left(\eta^{k+1} - 2\eta^k + \eta^{k-1}\right)}{\Delta t^2} - \frac{C_p^2(1-n)}{\omega^2}\frac{\left(\eta_{yy}^{k+1} - 2\eta_{yy}^k + \eta_{yy}^{k-1}\right)}{\Delta t^2}$$

$$= \frac{C_p^2(1-n)}{\omega^2}\frac{\left(\eta_{xx}^{k+1} - 2\eta_{xx}^k + \eta_{xx}^{k-1}\right)}{\Delta t^2} + C_p^2\left(\eta_{xx}^k + \eta_{yy}^k\right)$$

$$+ \left(nC_p^2\right)_x \eta_x^k + \left(nC_p^2\right)_y \eta_y^k + \frac{3}{2}g\left(3 - 2n - \frac{\omega^2 C_p^2}{g^2}\right)\left[\left(\bar{\eta}^k\bar{\eta}^k\right)_{xx} + \left(\bar{\eta}^k\bar{\eta}^k\right)_{yy}\right],$$

$$(13)$$

in which $\bar{\eta}^k = (\eta_{i,j+1}^k + \eta_{i,j}^k + \eta_{i,j-1}^k)/3$. η^{k+1} and η_{yy}^{k+1}'s appearing on the left-hand side are the only unknowns. The η^{k+1}'s obtained from (12) are only the first estimates, which are used on the right-hand side of (13) for improved computations. Since the x-direction is taken as the main wave propagation direction, equation (12) is solved once more using the updated new time values obtained from (13). In all the computational tests presented later further iterations brought no improvements so it was concluded that three sweeps (x, y, and x again) would be enough for most problems.

Equation (5) may likewise be manipulated into a computationally efficient form

$$n\eta_t + \frac{1}{2}C_p(1+n)\eta_x - \frac{C_p^2}{\omega^2}(1-n)\eta_{xxt} - \frac{C_p^3}{2\omega^2}(1-n)\eta_{xxx}$$

$$+ \frac{1}{2}\left[(C_p)_x + C_p n_x\right]\eta + \frac{3}{4}\frac{g}{C_p}\left(3 - 2n - \frac{\omega^2 C_p^2}{g^2}\right)\left(\eta^2\right)_x = 0,$$

$$(14)$$

where n and C_p are the only variables to be stored. Equation (14) yields an implicit scheme when three-time-level finite difference approximations are used for replacing the derivatives:

$$n\frac{\left(\eta^{k+1} - \eta^{k-1}\right)}{2\Delta t} - \frac{C_p^2}{\omega^2}(1-n)\frac{\left(\eta_{xx}^{k+1} - \eta_{xx}^{k-1}\right)}{2\Delta t}$$

$$= \frac{1}{2}C_p(1+n)\eta_x^k - \frac{C_p^3}{2\omega^2}(1-n)\eta_{xxx}^k + \frac{1}{2}\left[(C_p)_x + C_p n_x\right]\eta^k \quad (15)$$

$$+ \frac{3}{4}\frac{g}{C_p}\left(3 - 2n - \frac{\omega^2 C_p^2}{g^2}\right)\left(\bar{\eta}^k\bar{\eta}^k\right)_x.$$

Sample Simulations

The first simulation is linear wave propagation over a circular shoal. This experiment was designed and carried out by Ito and Tanimoto (1972) to test their numerical wave model. The shoal was constructed as concentric circles whose centers were located three wavelengths away from the incoming boundary. The width of the wave flume was $6L_o = 2.4$ m, where $L_o = 0.4$ m is the incident wavelength. Analytically, the water depth h may be expressed as

$$h = h_c + e_o r^2 \qquad \text{for} \qquad r < R$$

$$h = h_o \qquad\qquad \text{for} \qquad r \geq R$$

where

$$r^2 = (x - x_c)^2 + (y - y_c)^2,$$
$$e_o = (h_o - h_c)/R^2. \tag{16}$$

Here, $R = 2L_o$ is the shoal radius, $h_o = 0.15$ m the water depth outside the shoal, $h_c = 0.05$ m the water depth at the center of the shoal located at $(x_c = 3L_o, y_c = 3L_o)$. Thus, the depth to the wavelength ratio at the incoming boundary was $h_o/L_o = 0.375$, which reduced to $h_c/L_o = 0.125$ at the shoal center.

Ito and Tanimoto (1972) performed their experiments for three different incident wave height to wavelength ratios $H_o/L_o = 0.016$, 0.026, and 0.035. In the computations however, the selected wave height was immaterial because the linearized form of (11) was used. The computations were done with $\Delta x = L_o/10$, $\Delta y = L_o/6$, and $\Delta t = T/10$. Higher resolutions were found to be unnecessary as the results changed very little. An equally important point is the computational time which for this case was no more than a few minutes on a personal computer. This computational efficiency applied to nonlinear cases as well since the inclusion of nonlinearity amounts to only quasi-linear additions appearing on the right-hand sides of equations (12) and (13). A perspective view of the fully-developed wave field is depicted in figure 1, after 20 wave periods elapsed from the commencement of the computation.
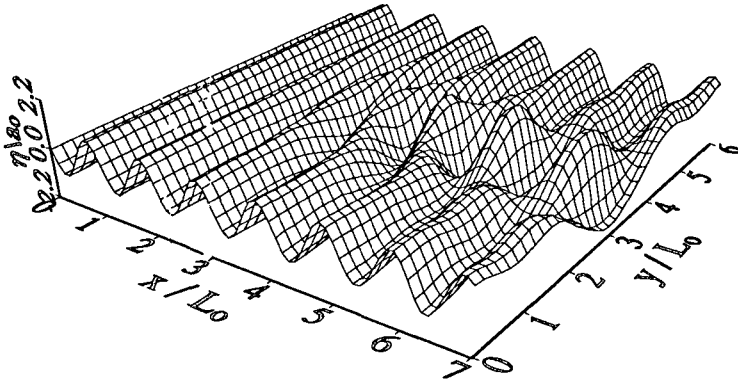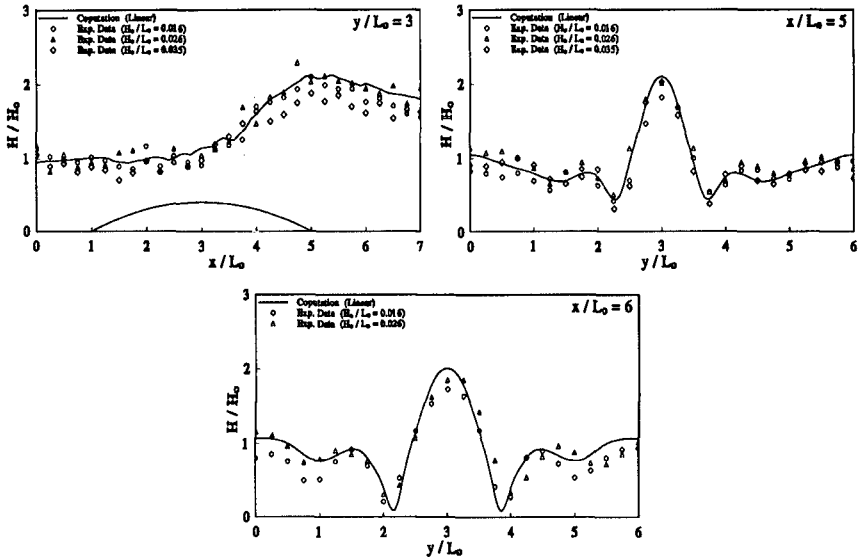

Figure 1: Perspective view of the fully developed wave field over a circular shoal.

In figures 2a, 2b, and 2c, the nondimensional wave height variations along the centerline and across the wave tank are compared with the measurements. As it is seen, the computational results agree remarkably well with the measurements.
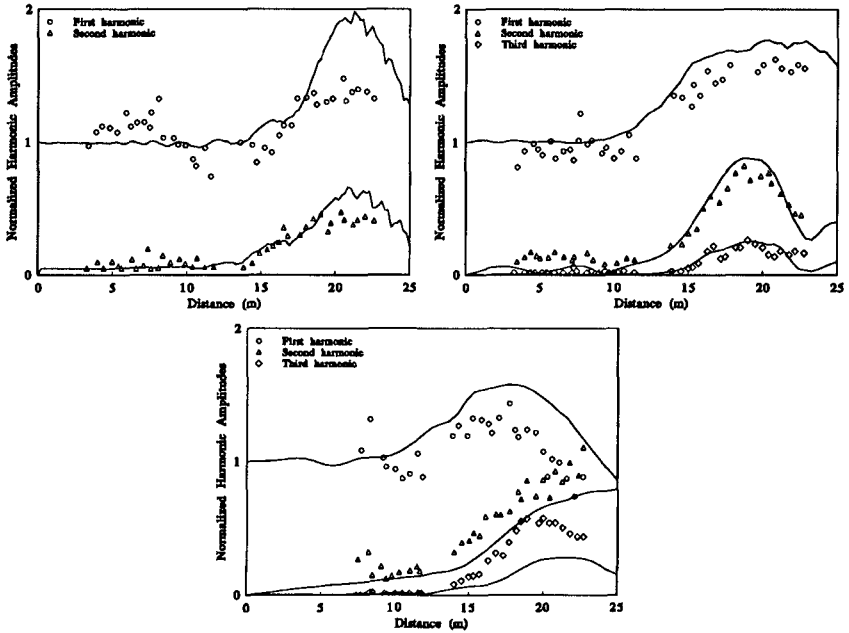

Figures 2a, b, c: Comparisons of the measured and computed wave-height variations along the centerline $y/L_o = 3$, across the wave tank at $x/L_o=7$ and at $x/L_o=6$.

The second case is the computation of wave convergence over a bottom topography that acts as a focusing lens (Whalin, 1972). The wave tank used in the experiments was 25.6 m long and 6.096 m wide. In the middle portion of the tank eleven semicircular steps were evenly spaced to form a topographical lens. The equations describing the topography are given in Whalin (1972).

Three sets of experiments were conducted by generating waves with periods $T = 1$, 2, and 3 seconds and the harmonic amplitudes along the centerline of the wave tank were measured at various stations. For all three cases the computations were performed with a span-wise resolution Δy of 1/10 of the wave tank width. Since the bathymetry is symmetric with respect to the centerline, only one-half of the tank is discretized. The no-flux boundary conditions are used along the centerline and the side-wall. Figure 3a compares the computed harmonic amplitudes with the measured data for the incident wave period $T = 1$ second and the wave amplitude $a_0 = 1.95$ cm. The time-step and the x-direction resolution were $\Delta t = T/25$ and $\Delta x = L_m/25$ with L_m denoting the mean wavelength computed as the average of the deep-water and shallow-water wavelengths. In figure 3b the case for $T = 2$ seconds and $a_0 = 0.75$ cm is shown, the resolutions were $\Delta t = T/30$ and $\Delta x = L_m/30$. Figure 3c gives the comparisons for $T = 3$ second waves with the deep water wave amplitude $a_0 = 0.68$ cm. Since the harmonic amplitudes were comparable with the primary wave amplitude, it was necessary to adopt somewhat higher resolutions and therefore $\Delta t = T/35$ and $\Delta x = L_m/35$ for this last case.

Figures 3a, b, and c show that the agreements of the computations with the measurements are not as good as the previous case; nonetheless the overall model predictions appear to be acceptable. For nonlinear directional waves, a better numerical approach is expected to yield better results, as the present numerical scheme has been observed to be sensitive (unlike the linear case) to the adopted resolution when the waves were nonlinear.

Figures 3a, b, c: Comparisons of the measured (scatter) and computed (solid line) harmonic amplitude variations along the centerline of the wave tank for $T = 1$ s (top left), $T = 2$ s (top right), and $T = 3$ s (bottom) waves.

To give an idea about the wave patterns, a perspective view of the fully-developed wave field is given in figure 4 for $T = 2$ second waves.
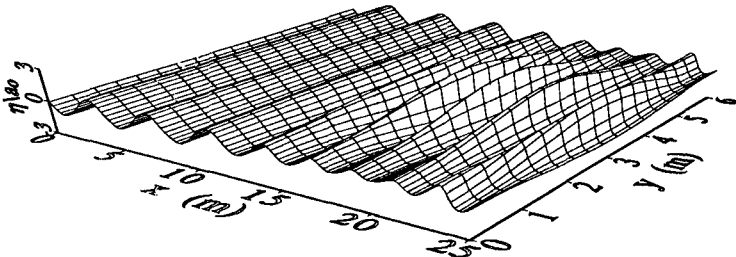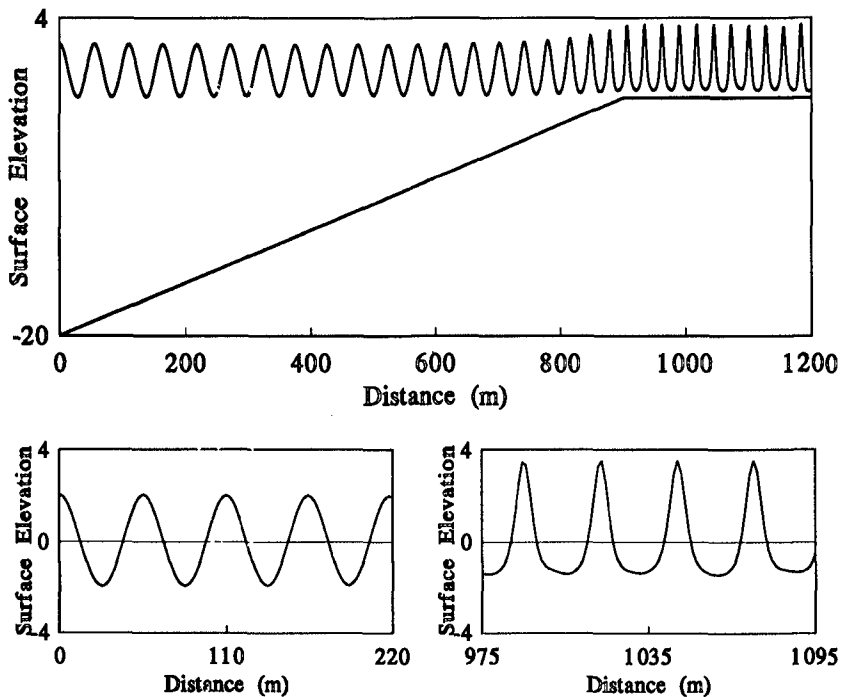

Figure 4: Perspective view of the fully-developed nonlinear wave field over a topographical lens ($T = 2$ s waves).

In order to demonstrate the wide applicable range of the proposed wave model we shall now consider the transformation of an initially second-order Stokes wave train into a cnoidal wave train over uniformly decreasing depth with a constant slope of 1:50. The water depth in the deep section is 20 m and after a distance of 900 m it reduces to 2 m. The incident wave is a second-order Stokes wave with $T = 6$ s and $kH_o = 0.1$. The initial steepness was chosen small so that an unacceptably large wave steepness in the shallowest region could be prevented.

The computations were done with $\Delta t = T/40$ and $\Delta x = L/40$. Figure 5a shows the spatial variation of the initially second-order Stokes wave as it propagates over the slope. In the deeper region the wave train does not yet feel the bottom so it travels without change of form for more than 500 m. Then, the finite- depth effect begins to steepen the waves. Finally, when the waves reach the shallowest region they are much steeper $H/h = 0.55$ and resemble to the cnoidal waves rather than the Stokes waves, as it can clearly be seen from the closer views given in the figures 5b and 5c. Indeed, the computations with the Stokes theory yields a very unacceptable wave form for this shallow depth as the theory virtually breaks down. Unlike the Stokes theory, the coefficients of the wave model adjusts properly according to the local depth hence enable the model simulate the proper wave form for the depth concerned.

Figures 5a, b, c: Transformation of an initially second-order Stokes wave train into a cnoidal wave train over a uniformly decreasing water depth. The two closer views show respectively the deep and shallow water regions. (Vertical scale is arbitrary.)

Concluding Remarks

Various forms of a recently proposed nonlinear refraction-diffraction model have been presented along with analytical investigations examining its nonlinear and dispersion characteristics. Sample simulations using the time-dependent nonlinear mild-slope equation and its unidirectional form have been performed. The proposed equations do not have any depth restriction and accommodate exact linear shoaling characteristics over mild-slopes so long as the incident wave frequency coincides with the specified dominant frequency of the wave model. The equations also include all the second-order nonlinear contributions and therefore can simulate the cnoidal waves and the Stokes waves with equal accuracy. The proposed equations may thus be regarded models for the combined nonlinear refraction-diffraction of waves over arbitrary depths. It is also worthwhile to emphasize that the applicability of the model equations is not limited to periodic waves; narrow-banded random waves may as well be simulated accurately.

Acknowledgment

References

Beji, S. and K. Nadaoka, 1997. A time dependent nonlinear mild-slope equation for water waves. *Proc. Roy. Soc. Lond. A*, **454**.

Beji, S. and K. Nadaoka, 1996. A formal derivation and numerical modelling of the improved Boussinesq equations for varying depth. *Ocean Engng.*, **23-8**: 691-704.

Berkhoff, J.C.W., 1972. Computation of combined refraction-diffraction. *Proc. 13th Int. Conf. Coast. Engng.*, 1: 471-490.

Byrne, R.J., 1969. Field occurrences of induced multiple gravity waves. *J. Geophys. Res.*, **74-10**: 2590-2596.

Fenton, J., 1972. A ninth-order solution for the solitary wave. *J. Fluid Mech.*, **53**: 257-271.

Freilich, M.H. and R.T. Guza, 1984. Nonlinear effects on shoaling surface gravity waves. *Philos. Trans. R. Soc. Lond. A*, **311**: 1-41.

Ito, Y. and K. Tanimoto, 1972. A method of numerical analysis of wave propagation-Application to wave diffraction and refraction. *Proc. 13th Int. Conf. Coast. Engng.*, 1: 503-522.

Madsen, P.A., R. Murray and O.R. Sørensen, 1991. A new form of the Boussinesq equations with improved linear dispersion characteristics. *Coastal Engng.*, **15**: 371-388.

Miles, J.W., 1980. Solitary waves. *Ann. Rev. Fluid Mech.*, **12**: 11-43.

Nadaoka, K., Beji, S. and Nakagawa, Y. 1994. A fully-dispersive nonlinear wave model and its numerical solutions. *Proc. 24th Int. Conf. Coast. Engng.*, 1: 427-441.

Nadaoka, K., Beji, S. and Nakagawa, Y. 1997. A fully-dispersive weakly-nonlinear model for water waves. *Proc. Roy. Soc. Lond. A*, **453**: 1-16.

Nwogu, O., 1993. Alternative form of Boussinesq equations for nearshore wave propagation. *J. Waterway, Port, Coastal, and Ocean Engng.*, **119-6**: 618-638.

Rayleigh, Lord, 1876. On waves. *Phil. Mag.*, **1**: 257-279.

Smith, R. and T. Sprinks, 1975. Scattering of surface waves by a conical island. *J. Fluid Mech.*, **72**: 373-384.

Young, I.R., 1989. Wave transformation over coral reefs. *J. Geophys. Res.*, **94**: 9779-9789.

Whalin, R.W., 1972. Wave refraction theory in a convergence zone. *Proc. 13th Int. Conf. Coast. Engng.*, **1**: 451-470.

Witting, J.M., 1984. A unified model for the evolution of nonlinear water waves. *J. Comp. Phys.*, **56**: 203-236.

Zabusky, N.J. and M.D. Kruskal, 1965. Interaction of solitons in a collisionless plasma and recurrence of initial states. *Phy. Rev. Lett.*, **15**: 240.